Articles

Two Crystal Structures of Human Neutrophil Collagenase, One Complexed with a Primed- and the Other with an Unprimed-Side Inhibitor: Implications for Drug Design†

Enrico Gavuzzo,[#] Giorgio Pochetti,[#] Fernando Mazza,*[,#,⊥] Carlo Gallina,[▽] Barbara Gorini,[§] Silvana D'Alessio,[||] Michael Pieper,[⊗] Harald Tschesche,[⊗] and Paul A. Tucker[‡]

Istituto di Strutturistica Chimica, CNR, C. P. n. 10, 00016 Monterotondo Stazione, Roma, Italy; Dipartimento di Chimica, Ingegneria Chimica e Materiali, Università degli Studi, V. Vetoio, 67010 L'Aquila, Italy; Dipartimento di Scienze del Farmaco, Università G. d'Annunzio, V. dei Vestini, 66100 Chieti, Italy; Centro di Studio per la Chimica del Farmaco del CNR, Università "La Sapienza", P. A. Moro 5, 00185 Roma, Italy; Polifarma Research Center, V. Tor Sapienza 138, 00185 Roma, Italy; Fakultät für Chemie, Abteilung Biochemie I, Universität Bielefeld, Universitätstrasse 25, D-33615 Bielefeld, Germany; and EMBL c/o DESY, Notkestrasse 85, Geb 25a, D-22603 Hamburg, Germany

Received November 26, 1999

Two crystal structures of human neutrophil collagenase (HNC, MMP-8), one complexed with a primed- and the other with an unprimed-side inhibitor, were determined using synchrotron radiation at 100 K. Both inhibitors contain non-hydroxamate zinc-binding functions. The Pro-Leu-L-$Trp^P(OH)_2$ occupies the unprimed region of the active site, furnishes new structural information regarding interaction between the catalytic zinc ion and the phosphonate group, and is the only example of occupation of the S_1 subsite of MMP-8 by the bulky tryptophan side chain. The *(R)*-2-(biphenyl-4-ylsulfonyl)-1,2,3,4-tetrahydroisochinolin-3-carboxylic acid, a conformationally constrained D-Tic derivative, accommodates its biphenyl substituent into the deep primary specificity S_1' subsite, inducing a widening of the entrance to this pocket; this modification of the protein, mainly consisting in a shift of the segment centered at Pro217, is observed for the first time in MMP-8 complexes. Cation−aromatic interactions can stabilize the formation of both complexes, and the beneficial effect of aromatic substituents in proximity of the catalytic zinc ion is discussed. The phosphonate group bound to either a primed- or unprimed-side inhibitor maintains the same relative position with respect to the catalytic zinc ion, suggesting that this binding function can be exploited for the design of combined inhibitors assembled to interact with both primed and unprimed regions of the active cleft.

Introduction

Matrix metalloproteinases (MMPs) are a family of zinc-dependent enzymes playing an important role in various physiological and pathological conditions. Although their precise functions are not yet completely understood, they seem to regulate the homeostasis of different tissues under the control of naturally occurring specific inhibitors of metalloproteinases (TIMPs). A misregulation between MMPs and TIMPs is implicated in a number of pathological states such as tumor metastasis,[1] multiple sclerosis,[2] and rheumatoid arthritis.[3] Therefore MMPs became attractive targets for the design and development of low-molecular-weight inhibitors[4] potentially useful as innovative therapeutic agents for treating the above diseases. Most synthetic inhibitors of MMPs are formed by a zinc-binding function and a peptide or peptidomimetic backbone, assembled to ensure cooperative binding interactions with both the catalytic zinc ion and the adjacent specificity subsites of the enzyme. The majority of the more powerful synthetic inhibitors incorporate hydroxamate group as the zinc-binding function. Hydroxamate inhibitors, however, show lack of selectivity and are toxic.

In this context, the search for non-hydroxamate zinc-chelating groups which combine binding interactions at both the primed and unprimed regions of MMPs is useful. In fact, chronic toxicity arising from metabolic degradation to hydroxylamine, a known carcinogenic compound,[5] is avoided. Moreover, placing the zinc-binding function internal to the ligand backbone allows occupation of a larger number of subsites, and consequently, inhibitor selectivity is enhanced. In this regard phosphinic chemistry allows the development of transition-state analogues capable to interact on both sides of the catalytic zinc ion. An example has been reported

† Preliminary communication of this work has been presented during the PX-day, Feb 8, 1999, held at IRBM, Pomezia, Roma, Italy. Abbreviations: FLTP, *N*-[(furan-2-yl)carbonyl]-Leu-L-$Trp^P(OH)_2$; MMP-1, fibroblast collagenase; MMP-2, gelatinase A; MMP-3, stromelysin; MMP-8, human neutrophil collagenase; MMP-9, gelatinase B; PLGNHOH, Pro-Leu-Gly-NHOH; PLTP, Pro-Leu-L-$Trp^P(OH)_2$; Tic, 1,2,3,4-tetrahydroisochinolin-3-carboxylic acid.

* Corresponding author. Tel: 0039-06-90625142. Fax: 0039-06-90672630. E-mail: mazza@isc.mlib.cnr.it.

[#] CNR.

[⊥] Università degli Studi, L'Aquila.

[▽] Università G. d'Annunzio.

[§] Università "La Sapienza".

[||] Polifarma Research Center.

[⊗] Universität Bielefeld.

[‡] EMBL c/o DESY.

10.1021/jm9909589 CCC: $19.00
Published on Web 08/12/2000

in the study of astacin complexed with the phosphinic inhibitor Z-Pro-Lys-PheΨ(PO_2CH_2)-Ala-Pro-OMe.[6] Very recently it has been shown that substitution at both P_1' and P_2 positions of phosphinic pseudopeptides of the general formula R-Xaa-Ψ(PO_2CH_2)-Xaa′-Yaa′-NH_2 can contribute to the design of inhibitors capable of selectively blocking some MMPs.[7] The determination of the mode of binding of shorter primed- and unprimed-side inhibitors complexed with MMPs is therefore useful for acquiring a detailed knowledge of the enzyme subsites and of the local arrangement of the ligand peptide chains. Here we report two crystal structures of a primed- and unprimed-side inhibitor complexed in the active site of the catalytic domain of human neutrophil collagenase (HNC).

The unprimed-side inhibitor derives from our recent studies[8] where we have modified endogenous tripeptides acting as weak and competitive inhibitors of reprolysins, to obtain novel types of more powerful inhibitors. The *N*-[(furan-2-yl)carbonyl]-Leu-L-$Trp^P(OH)_2$ (FLTP) phosphonate inhibitor was about 100-fold more potent than the carboxylate analogue against adamalysin II,[9] a zinc proteinase structurally related to MMPs. Both crystal structures of adamalysin II complexed with FLTP[8] and its carboxylate analogue[10] show that the phosphonate and carboxylate groups bind the catalytic zinc ion, while their peptide backbones adopt a similar but unusual retrobinding mode in the primed region. Further chemical modifications, obtained by replacing the furan ring of FLTP with pentatomic heterocyclic aromatic and nonaromatic rings, led to new phosphonate analogues whose inhibitory activities were evaluated against adamalysin II, MMP-2, MMP-3, MMP-8, and MMP-9.[11] Among these, the Pro-Leu-L-$Trp^P(OH)_2$ analogue (PLTP) exhibits an interesting increase of affinity against MMP-8 and MMP-9, whereas its potency against adamalysin II decreases. We, therefore, wanted to determine the mode of binding of this inhibitor at the active site of MMP-8 and performed the X-ray structure determination of the complex.

The primed-side inhibitor is *(R)*-2-(biphenyl-4-ylsulfonyl)-1,2,3,4-tetrahydroisochinolin-3-carboxylic acid.[12,13] This simple D-Tic[14−21] derivative (TIC) attracted our attention because of its nanomolar inhibitory activity against HNC, despite the following unfavorable features: (i) 1,3-bidentate or monodentate zinc binding by the carboxylate group which is generally weaker than the 1,4-bidentate hydroxamate group;[22] (ii) lack of peptide groups, generally engaged in H-bonds with the enzyme active site, thus providing a reduced number of interactions compared to di- and tripeptide hydroxamates; and (iii) noncomplementarity with the collagenase extended binding region, due to the constrained folded conformation of the sulfonamide junction which is populated only by *gauche* conformers.[23−26] While our work was in progress, the crystal structure of this inhibitor complexed with a differently truncated form of MMP-8 (Gly99−Glu271) was reported[27] and validated the docking calculations performed on a large series of Tic derivatives in the catalytic domain of MMP-8. Here we report our X-ray structure results at the higher resolution of 1.2 Å and describe the implications of our detailed investigation on drug-binding and design studies.

Scheme 1

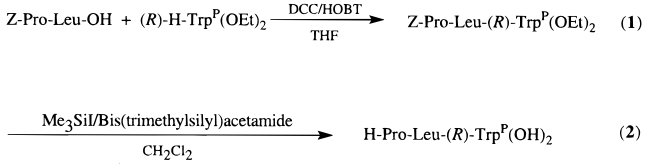

Results

Synthesis. Several phosphorus-containing peptidomimetics[28] have been synthesized following isolation of phosphoramidon, a natural inhibitor of thermolysin and other metalloproteinases. The tripeptide phosphonate **2** was obtained according to Scheme 1, following standard procedures[29,30] with minor modifications. Z-Pro-Leu-L-$Trp^P(OEt)_2$ (**1**) was prepared by coupling of Z-Pro-Leu-OH with L-phosphotryptophan diethyl ester[31] by the DCC/HOBT method.[29] Hydrolysis of the diethyl phosphonate and removal of the benzyloxycarbonyl group were achieved by treatment with trimethylsilyl iodide in the presence of bis-trimethylsilyl acetamide to give the desired phosphonate **2**.

Crystal Structure of the Complex MMP-8:PLTP. The peptide backbone of the phosphonate inhibitor occupies the unprimed region, there adopting an almost extended conformation running antiparallel to the edge strand of MMP-8, as shown in the $2F_o - F_c$ electron density map (Figure 1). The electron density of the Trp side chain is not well-defined toward the periphery, indicating mobility probably caused by the shallow concavity of the S_1 subsite that is solvent-exposed. After PLGNHOH,[32−34] PLTP is the second example of an unprimed-side inhibitor complexed at the MMP-8 active site and the first with the phosphonate group approaching the catalytic zinc ion from the unprimed region. Figure 2 shows the main interactions characterizing the binding of the inhibitor. The two phosphonate oxygens O_1 and O_2 bind the catalytic zinc ion in an asymmetric bidentate mode. O_1 can also engage both oxygens of Glu198 in H-bonding, and O_3 can form further H-bonds as shown in Figure 2. The Trp side chain partly fits into the S_1 concavity, where both methyl groups of Ile159 point toward the aromatic π cloud. This represents the first example of an inhibitor side chain occupying the MMP-8 S_1 subsite, since the other unprimed-side inhibitor PLGNHOH contains Gly which lacks the side chain as P_1 residue. The Pro-Leu segment of the phosphonate inhibitor interacts in a similar mode to that of PLGNHOH; the Leu side chain adopts the different $g^-(t,g^-)$ conformation, allowing each methyl group to point toward the two rings of His201 and His207. The inhibitor Pro residue fits into the S_3 subsite, stacking its pyrrolidine ring onto that of Phe164, and the distance between the Pro N atom and the center of the Phe ring is 4.4 Å.

Crystal Structure of the Complex MMP-8:TIC. Figure 3 shows the $2F_o - F_c$ electron density map of the D-Tic inhibitor, while a scheme of the main interactions characterizing its binding is presented in Figure 4. The axial carboxylate group of the inhibitor ligates the catalytic zinc ion in an asymmetric bidentate mode. This coordination resembles that found in the crystals of MMPs complexed with *N*-carboxyalkyl dipeptides[35,36] but differs from the symmetric bidentate mode of

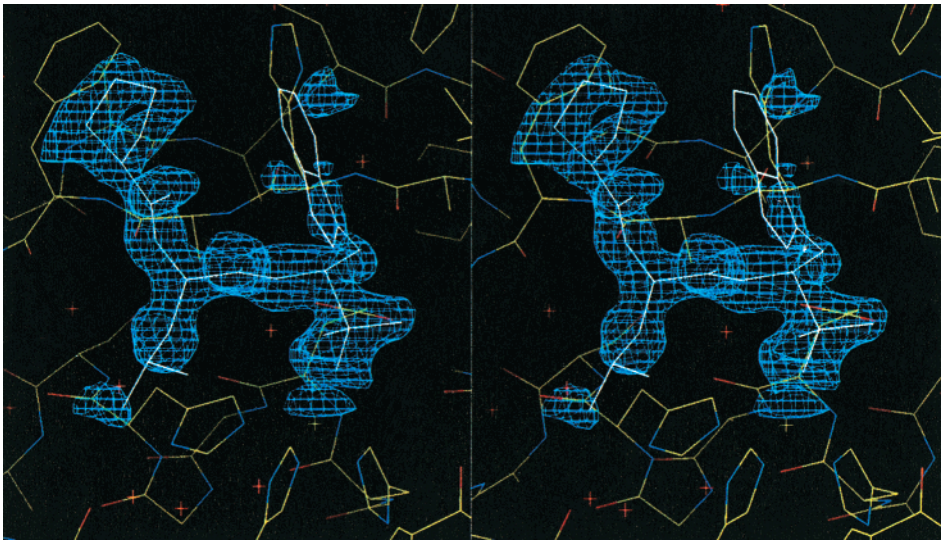

Figure 1. Stereoview of the $2F_o - F_c$ electron density at the active site of MMP-8 with the PLTP refined model superimposed. The map is contoured at 1.5σ.

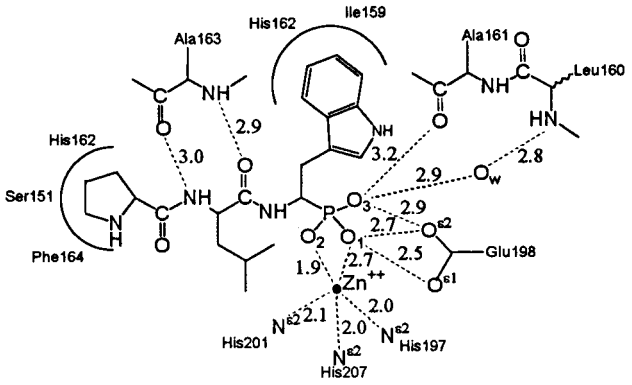

Figure 2. Schematic representation of the binding interactions (dashed lines) of the inhibitor PLTP at the active site of MMP-8. The distances are reported in Å.

ligation realized by both Pol647 and Pol656 carboxylates in the active site of adamalysin II.[10] The oxygen O_2 can also form H-bonds with both oxygens of Glu198 and with the Ala163 NH group through a water bridge. The D-Tic residue protrudes out of the binding region and is mainly exposed to the solvent. It covers the cavity of the catalytic zinc ion, and the distance between the center of the π orbital and the metal is 5.0 Å. Both sulfonic oxygens are engaged in H-bonds. The O_3 interacts through a water bridge with the Gly158 CO group, and the O_4 forms a bifurcated H-bond with the NH groups of Leu160 and Ala161. It is worth noting that, among the four H-bonds normally anchoring substrate-like inhibitors to the primed region of MMP-8,[32−34,37−40] the one formed with the NH of Leu160 is always conserved. The biphenyl group is properly directed by the conformationally restricted g^- sulfonamide junction into the deep primary specificity pocket S_1' where it is completely buried. The π orbital of its first aromatic ring, bound to the sulfonamide junction, is 4.8 Å from the catalytic zinc ion. Previous studies reported the ability of MMP-3 to accommodate aromatic moieties in the S_1' pocket,[41] where even simple biphenyl derivatives weakly bind as shown by SAR and NMR data.[42]

Discussion

The Phosphonate Zinc-Binding Function. The crystal structures of FLTP complexed with adamalysin II[8] and PLTP complexed with MMP-8 allow a comparison of the geometry of interaction between the phosphonate groups bound to a primed- and unprimed-side inhibitor. While the phosphonate group ligates the metal ion in an asymmetric bidentate mode, maintaining the same angles in both cases, the values and number of atomic contacts, reported in Table 1, are different. In particular, all the Zn···O and O···O contacts of the first column of Table 1 are shorter than those of the other column. The third phosphonate oxygen O_3 of PLTP can be engaged in two additional H-bonds with the protein, while in the case of FLTP, there is only one H-bond with a water molecule. Considering the structural similarity at the catalytic site of the two enzymes, the present data show that the protein−phosphonate interaction realized by the unprimed-side inhibitor is stronger than that for the primed-side inhibitor. A superposition of some structural elements common to the two proteins, shown in Figure 5, reveals that the phosphorus and two oxygen atoms of the two phosphonate groups practically overlap, whereas a switching occurs between the third oxygen of one group and the α-carbon atom of the other group. This allows the elongation of the peptide chain toward the primed or unprimed region of the active site, respectively.

Cation−Aromatic Interactions. Electrostatic interactions between the positive charge of a cation and the negative partial charge of aromatic π clouds have been proposed in molecular recognition processes and recently explored by experimental and theoretical works.[43−47] A physical model of this interaction has been reported in a review.[46]

In both crystal structures of the present work, the position adopted by some aromatic rings suggests that similar interactions may be present and cooperate to the stabilization of the complexes. In the MMP-8:PLTP adduct, the inhibitor Pro ring stacks onto the Phe164 aromatic π cloud of the enzyme. The amino group of the pyrrolidine ring, probably protonated at the pH of investigation and in the crystal, can be involved in an

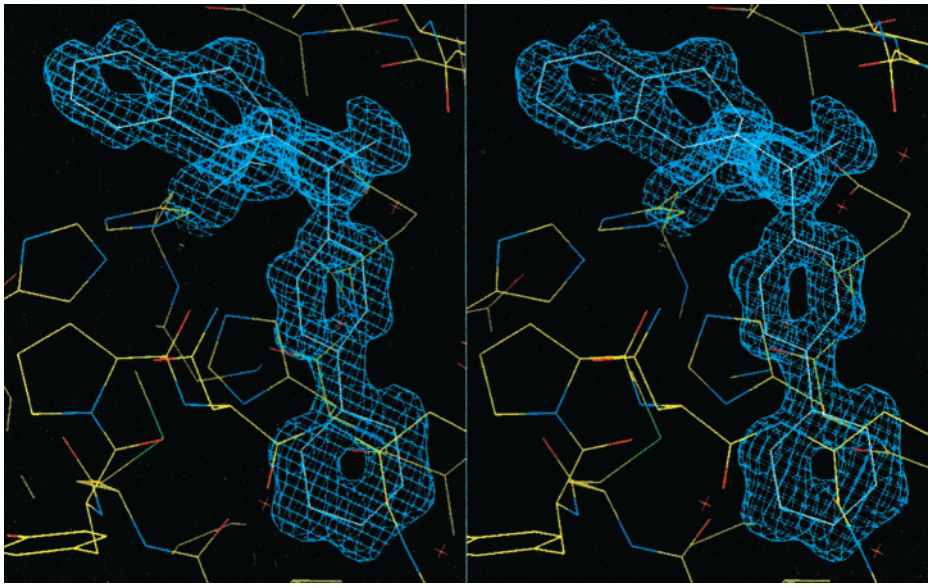

Figure 3. Stereoview of the $2F_o - F_c$ electron density at the active site of MMP-8 with the TIC refined model superimposed. The map is contoured at 1.7σ.

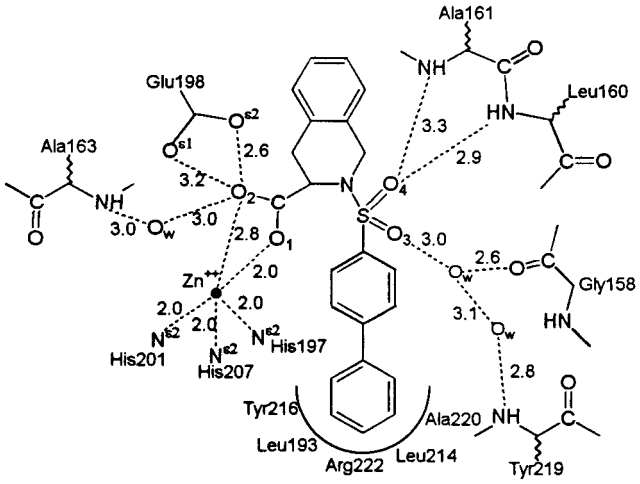

Figure 4. Schematic representation of the binding interactions (dashed lines) of the TIC inhibitor at the active site of MMP-8. The distances are reported in Å.

Table 1. Main Contacts (Å) Formed by the Phosphonate Group with the Active Site in the Crystal Complexes MMP-8:PLTP and Adamalysin:FLTP

MMP-8:PLTP		adamalysin:FLTP	
Zn−N$^{\epsilon}$2(197)	2.0	Zn−N$^{\epsilon}$2(142)	2.1
Zn−N$^{\epsilon}$2(201)	2.1	Zn−N$^{\epsilon}$2(146)	2.2
Zn−N$^{\epsilon}$2(207)	2.0	Zn−N$^{\epsilon}$2(152)	2.3
Zn−O_1	2.7	Zn−O_1	2.8
Zn−O_2	1.9	Zn−O_2	2.0
O_1−O$^{\epsilon}$1(198)	2.5	O_1−O$^{\epsilon}$1(143)	2.9
O_1−O$^{\epsilon}$2(198)	2.7	O_1−O$^{\epsilon}$2(143)	3.2
O_3−O$^{\epsilon}$2(198)	2.9		
O_3−O(161)	3.2		

attractive electrostatic interaction with the π cloud of Phe164 ring centered at 4.5 Å from the cation. In the MMP-8:TIC, two aromatic rings of the inhibitor cluster the catalytic zinc ion at 4.8 and 5.0 Å from their centers. A similar interaction involving the catalytic zinc ion has been already described for the complex between MMP-8 and batimastat,[38] where the thiophene aromatic ring of the inhibitor faces the cation at a distance of 4.5 Å. We believe that the contribution of these attractive electrostatic interactions, even at relatively large distances, should not be neglected in the evaluation of the stabilization of the complexes and could be taken into account in the design of MMP inhibitors.

Induced Conformational Change of the S_1' Entrance and Ligand Conformational Preorganization. The high-resolution crystal structure of the complex MMP-8:TIC allows us to evaluate the conformational changes in the bottleneck entrance of the S_1' pocket induced by the sulfonamide inhibitor. We have calculated the distance between the carbonyl oxygens of Ala161 and Pro217, the two residues at the upper and lower sides, respectively, of the entrance (see Figure 6), for all reported MMP-8 crystal complexes[32−34,37−40] and found it to be close to 8.0 Å, whereas a significant increase to 8.8 Å was found for the MMP-8:TIC complex. The widening of this entrance mainly involves the lower side segment, since the upper side is formed by β-sheets interconnected by several H-bonds. A superposition of the MMP-8:TIC complex with the unmodified form of MMP-8, as found in the MMP-8:PLTP complex, is shown in Figure 6. For the sequence Tyr216-Pro217-Asn218 in MMP-8:TIC the backbone atoms are shifted more than 0.5 Å, relative to the corresponding residues in MMP-8:PLTP. This conformational change allows the accommodation of the biphenyl group into the S_1' pocket. In fact, the carbonyl oxygen of Pro217 of the unmodified MMP-8 would make unacceptable nonbonded contacts of 2.6 and 2.3 Å with C_2 and C_3, respectively, of the internal phenyl ring of the biphenyl sulfonamide. These contacts are increased to 3.3 and 3.0 Å, respectively, in the modified form of MMP-8. Though this is the first observation of a significant change in the conformation of a segment of MMP-8, additional evidence for the flexibility of the same region in a metalloproteinase comes from the crystal structure of MMP-1 complexed with a *N*-(arylsulfonyl)-α-amino *N*-hydroxyamide.[48]

The D-Tic inhibitor, although possessing the weaker carboxylate zinc-binding function and a reduced number of H-bonding groups, induces a conformational modification of the protein, requiring additional energy. To account for its low K_i value, the entropic advan-

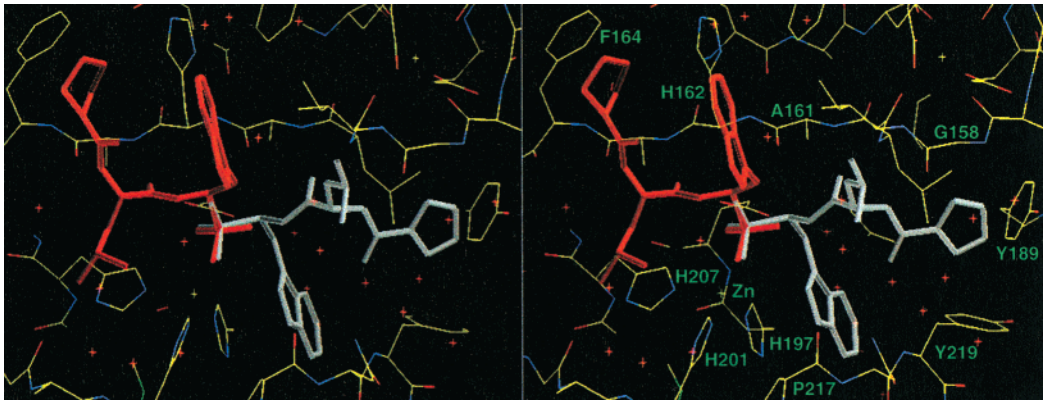

Figure 5. Stereoview of the superposition between the MMP-8:PLTP complex (MMP-8, yellow; PLTP, red) and the FLTP inhibitor (white) as found in the crystal complex with adamalysin II. The superposition was obtained by least-squares fitting the three N atoms of the histidines involved in zinc ligation and the zinc ions of the two enzymes. The central part shows the overlap of the PO_2^- anion common to both phosphonates. For clarity a few residues are labeled.

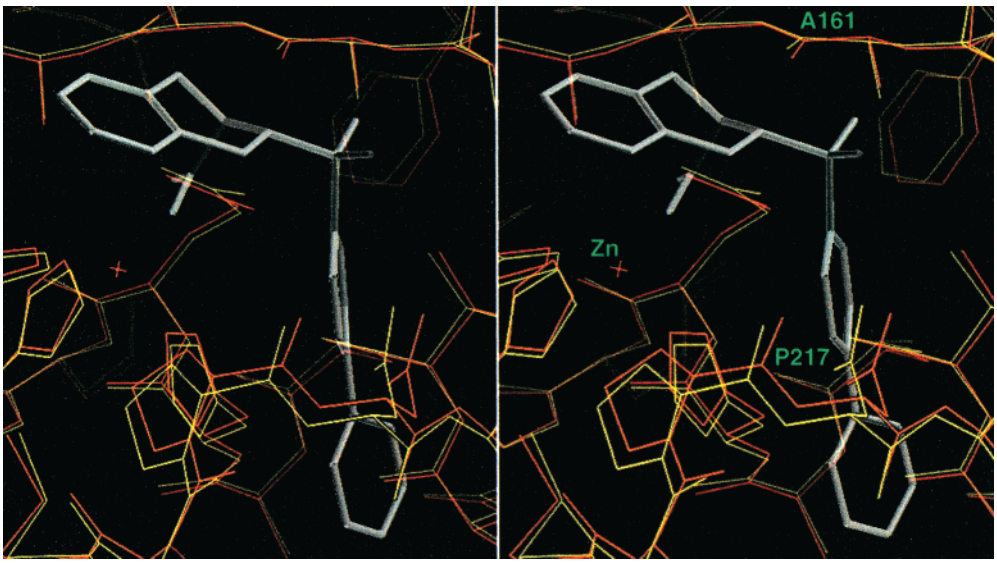

Figure 6. Stereoview of the superposition between the MMP-8:TIC complex (protein, yellow; inhibitor, white) and the unmodified form of MMP-8 (red) taken from the MMP-8:PLTP complex. The superposition was obtained by least-squares fitting the C^α atoms of the three histidines involved in zinc ligation, the catalytic zinc ions, and the C^α atoms of the sequence 159−164 of the upper rim of the active cleft. The lower part shows the displacement between the segments of the lower rim including Pro217. The residues Ala161 and Pro217 are labeled.

tage deriving from the conformational constraints present in this inhibitor should be considered. The restrictions involve: (i) the D-Tic residue, a Phe analogue showing only g^- rotamers for χ^1 and orientation of the aromatic ring almost perpendicular to that preferred[49] by Phe, Tyr, and Trp; (ii) the g^- sulfonamide junction[23−26] properly directing the biphenyl group into the deep S_1' pocket; and (iii) the biphenyl group adopting an average dihedral angle of about 30° between the two rings.[50]

PLTP Binding at the S Region of MMP-8. FLTP and PLTP are very similar, yet the binding of FLTP to adamalysin[8] greatly differs from that of PLTP to MMP-8. Although the active sites of the two enzymes are strictly related,[51] some differences in their S_3 and S_1' subsites may explain preferential binding of PLTP to the S region of MMP-8. The PLTP fits its Pro ring between those of His162 and Phe164 which form the S_3 small hydrophobic cleft of MMP-8 (see Figure 5). The S_3 subsite of adamalysin is lined by Lys110 and Tyr112, and the Tyr ring is bent far away from that of Phe in MMP-8. Therefore both hydrophobic and cation−π interactions with the P_3 Pro ring in the S region of a putative adamalysin:PLTP complex would be strongly reduced. Moreover, the bottleneck entrance of the S_1' pocket of MMP-8 (≅8.0 Å, above cited) is smaller than that of adamalysin (≅8.6 Å). This small shrinkage does not necessarily prevent the accommodation of the indole ring since HNC can still hydrolyze substrates containing Trp at P_1'.[52−54] Possible restrictions due to the adjustment of the phospho-Trp indole ring in the S_1' pocket of MMP-8 may decrease cooperativity of other binding interactions and therefore the affinity of the ligand. It should also be observed that the indole ring of FLTP in the S_1' pocket of adamalysin adopts $\chi^2 \cong 0°$.[8] This is a highly strained conformation since natural aromatic amino acids adopting $\chi^2 \cong 0°$ have never been observed in oligopeptides crystal structures.[49] At variance, the orientation of the indole ring of PLTP in the S_1 subsite of MMP-8 is practically perpendicular to that adopted by the same residue in the S_1' pocket of adamalysin. Thus, the lack of interaction with the primary spcificity subsite S_1' is, at least in part, counterbalanced by the absence of torsional strain at the Trp side chain of

PLTP. Finally, preferential binding of PLTP to the S region of MMP-8 can also be favored by the stronger interaction between the catalytic site and the phosphonate group approaching the zinc ion from the unprimed side, as above-discussed.

Conclusion

The prevailing interest in the design and study of MMP inhibitors with a hydroxamate zinc-binding function reflects the stronger chelating capacity of this group compared to other functional groups. An interesting example of inhibitors combining zinc chelation by hydroxamate with a peptide chain binding both the S and S′ subsites of the target enzyme has been recently presented.[55] There, the zinc-chelating function has been placed as close as possible to the peptide backbone, but it is not part of the backbone. Its free rotation around the bond connecting the hydroxamate to the peptide chain may be detrimental for binding because of a negative entropic effect. In this respect the design of inhibitors using a phosphinate chelating group included in the peptide backbone seems to be more convenient. The data here reported (see Figure 5) indicate that the PO_2^- anion, involved in zinc chelation by the two phosphonate inhibitors FLTP and PLTP, maintains the same relative position with respect to the catalytic zinc ion in both complexes. This finding represents an important experimental achievement. Combined phosphinic inhibitors may be modeled in the active site of different MMPs starting from the coordinates of this key PO_2^- chelating group. Moreover, peptidomimetic chains extending from the key PO_2^- phosphinic group toward both S and S′ regions of the active site can be designed on the basis of the arrangement assumed by shorter ligands. Additional indications deriving from the crystal structure of MMP-8:TIC, with optimal occupancy of the S_1' pocket by the biphenyl group and further beneficial effect of cation−aromatic interactions occurring in the same complex, can be considered in the design of combined inhibitors. The loss of potency due to the use of a weaker chelating group could be compensated by the increase of favorable contacts with the protein, since these inhibitors can span up to six subsites of the active cleft. In addition, since subsites of different MMPs are generally similar but not identical, it is expected that more selective phosphinic inhibitors can be obtained due to the increase of contacts involved.

Experimental Section

Synthesis of the Inhibitor. Commercial available reagents and solvents were purchased from Fluka or Aldrich and used with no additional purification. Melting points (Büchi oil bath apparatus) are uncorrected. IR spectra were obtained with a Perkin-Elmer 16 FPC FT-IR spectrophotometer. ^{1}H NMR spectra were recorded on a Varian XL-300 spectrometer using TMS as internal standard. $[\alpha]_D$ values were determined with a Schmidt-Haensch 1604 digital polarimeter. HPLC was performed with a Waters apparatus equipped with an UV 684 detector.

Z-Pro-Leu-L-Trp^P(OEt)$_2$ (1). To a solution of Z-Pro-Leu-OH (441 mg, 1.35 mmol) and (*R*)-phosphotryptophan diethyl ester (468 mg, 1.35 mmol) in anhydrous THF (7 mL) at 0 °C was added a solution of DCC (279 mg, 1.35 mmol) and HOBT (18 mg, 0.135 mmol) in the same solvent dropwise, under stirring. After standing at room temperature overnight, *N*,*N*′-dicyclohexylurea was filtered off and the solution concentrated under reduced pressure. The residue was dissolved in AcOEt (40 mL) and washed with saturated solution of $NaHCO_3$ and brine. The AcOEt solution was dried over Na_2SO_4 and the solvent removed under reduced pressure. When the oily residue was dissolved in anhydrous Et_2O, pure Z-Pro-Leu-(*R*)-Trp^P(OEt)$_2$ crystallized as a colorless hygroscopic solid: 570 mg (65%); $[\alpha]^{22}_D$ −74° (*c* 1.0, CH_3OH); IR (KBr) 3477, 2991, 1687, 1500, 1357, 1217, 1052 cm^{-1}; ^{1}H NMR (DMSO-d_6) δ 0.80 (m, 6H, Leu CH_3), 1.10−1.51 (m, 9H, CH_3−CH_2−O, Leu CH and Leu CH_2), 1.52−2.05 (m, 4H, Pro β and γCH_2), 3.00−3.50 (m, 4H, Pro δCH_2 and Trp^P CH_2), 4.00−4.20 (m, 5H, CH_3−CH_2−O and Pro αCH), 4.40 (m, 1H, Leu αCH), 4.80 (m, 1H, Trp^P αCH), 5.07 and 5.20 (A and B of an AB system, J = 12 Hz, 2H, benzyl CH_2), 6.69 (d, 1H, J = 8.1 Hz, Leu NH), 6.92−7.60 (m, 11H, indole, C_6H_5 and Trp^P NH), 8.81 (s, 1H, indole NH). Anal. ($C_{33}H_{45}N_4O_7P\cdot 2/3H_2O$) C, H, N.

H-Pro-Leu-L-Trp^P(OH)$_2$ (2). To a solution of Z-Pro-Leu-L-Trp^P(OEt)$_2$ (**1**) (550 mg, 0.86 mmol) in anhydrous CH_2Cl_2 (10 mL), under nitrogen, was added an excess (2.3 mL, 9.46 mmol) of bis(trimethylsilyl)acetamide under stirring. After 1 h at room temperature, the reaction mixture was cooled to −20 °C and an excess (0.23 mL, 6.88 mmol) of iodotrimethylsilane was added dropwise. The solution was allowed to warm to room temperature within 1 h and after 2 h it was concentrated under reduced pressure. The brown oily residue was taken up with 7:3 CH_3CN−H_2O (3 mL). After removal of the solvents under reduced pressure, the solid residue was washed with AcOEt and purified by semipreparative HPLC (Waters C18 Deltapack 19 × 300 mm column, 70:30 H_2O−CH_3CN, flow rate 9 mL/min, retention time 10.34 min). Removal of the solvent under reduced pressure and drying in high vacuum gave the pure product as an hygroscopic white solid: 200 mg (48%); $[\alpha]^{22}_D$ −97° (*c* 1.0, 1 N NaOH); IR (KBr) 3357, 3262, 2959, 1642, 1135, 1071 cm^{-1}; ^{1}H NMR (NaOD, D_2O) δ (H_3C−CO−CH_3 as internal standard at 2.2 ppm) 0.69 and 073 (2d, J = 7 Hz, 6H, Leu CH_3), 0.96−2.12 (m, 7H, Leu CH, Leu CH_2, β and γPro CH_2) 2.78−3.03 (m, 3H, Pro δCH_2 and 1H of Trp^P CH_2), 3.32 (m, 1H, Trp^P CH_2), 3.67 (m, 1H, Pro αCH), 4.03−4.30 (m, 2H, Leu αCH) and Trp^P αCH), 7.08−7.78 (m, 5H, indole). Anal. ($C_{21}H_{31}N_4O_5P\cdot 2H_2O$) C, H, N.

Purification of the Catalytic Domain of HNC. The truncated form Met80−Gly242 of the catalytic domain of HNC was expressed in *E. coli* and renaturated by dializing the inclusion bodies, which were solubilized in 6 M urea/100 mM 2-mercaptoethanol, against a buffer containing 100 mM NaCl, 5 mM $CaCl_2$, 0.5 mM $ZnCl_2$, 5 mM Tris/HCl, pH 7.5, as previously described.[56] The activated enzyme was subsequently purified to apparent homogeneity by hydroxamate affinity chromatography as judged by SDS−PAGE.

Crystallizations. Crystallizations were performed by hanging-drop vapor diffusion at 18 °C. Hanging droplets were made by mixing 2 μL of protein solution (6 mg/mL protein in 5 mM $CaCl_2$, 100 mM NaCl, 0.5 mM $ZnCl_2$, 3 mM MES-NaOH, 0.02% NaN_3, pH 6.0), 1 μL of inhibitor solution (20 mM inhibitor in 0.2 M MES-NaOH, 0.02% NaN_3, pH 6.0) and 5 μL of PEG solution (10% (m/v) PEG 6000, 0.2 M MES-NaOH, 0.02% NaN_3, pH 6.0). Droplets were concentrated against a reservoir buffer containing 2.0 M sodium phosphate buffer, 0.02% NaN_3, pH 6.0.

Data Collection. X-ray data were collected under cryogenic conditions (100 K) at the EMBL outstation, DESY, Hamburg, Germany, using a wavelength of 0.8345 Å and a 345 MAR Research image-plate scanner as detector. Before mounting in the nitrogen stream, the crystal was transferred into mother solution containing 35% PEG 400 for few seconds, then mounted in a rayon loop and flash-frozen. Data sets were collected at different resolutions up to the limit of 1.40 and 1.20 Å for the complexes MMP-8:PLTP and MMP-8:TIC, respectively. Data were integrated and scaled using the programs DENZO and SCALEPACK.[57] A summary of data collection and processing is given in Table 2.

Structure Analysis. The structure of MMP-8 complexed with PLGNHOH (diffraction data at 298 K, PDB code 1JAP) was used as starting model. Randomly about 5% of all reflections not included in the refinement were set aside for

Table 2. Data Collection and Processing

	MMP-8:PLTP	MMP-8:TIC
wavelength (Å)	0.8345	0.8345
crystal dimensions (mm)	0.21; 0.002; 0.01	0.38; 0.06; 0.02
temperature (K)	100	100
space group	$P2_12_12_1$	$P2_12_12_1$
cell dimensions (Å)	32.98; 68.67; 70.49	32.99; 68.68; 70.58
no. of processed intensities	106034	411807
no. of unique reflections	30229	50709
resolution range (Å)	30.0−1.40 (1.42−1.40)[a]	20.0−1.20 (1.22−1.20)[a]
completeness (%)	93.3 (85.6)[a]	99.3 (95.3)[a]
R_{sym}	0.081 (0.258)[a]	0.090 (0.177)[a]
$\langle I/\sigma(I)\rangle$	11.5 (4.1)[a]	19.6 (5.0)[a]

[a] The values in parentheses refer to the outer shell.

Table 3. Refinement Statistics

	MMP-8:PLTP	MMP-8:TIC
resolution range (Å)	10.0−1.40	10.0−1.20
no. of reflections	28619	48054
no. of protein atoms	1283	1283
no. of metal ions	4	4
no. of inhibitor atoms	31	28
no. of water molecules	281	271
rmsd bonds (Å)[a]	0.008	0.009
rmsd angles (deg)[a]	1.030	1.589
R for $F > 4\sigma$ (%)[b]	11.7	12.6
R for all data (%)[b]	13.4	12.9
R_{free} for $F > 4\sigma$ (%)[b]	17.9	16.5
R_{free} for all data (%)[b]	19.4	17.1
data/parameters[b]	2.0	3.3
goodness of fit[b]	2.7	1.8
Mean Isotropic Equivalent B (Å^2)		
protein atoms	13.6 (4.8−80.8)[c]	12.5 (5.1−76.9)[c]
metal ions	8.4 (7.6−8.9)[c]	7.7 (7.0−8.8)[c]
inhibitor atoms	32.1 (13.8−69.0)[c]	13.7 (8.0−24.9)[c]
water oxygens	32.8 (8.7−76.4)[c]	30.2 (6.5−63.6)[c]
Ramachandran Population		
favored regions (%)	90.6	91.3
allowed regions (%)	9.4	8.7

[a] Calculated by X-PLOR. [b] Calculated by SHELXL. [c] Highest and lowest B values are reported in parentheses.

cross-validation analysis by means of R_{free}. After several cycles of positional refinement by XPLOR,[58] followed by isotropic refinement of individual B factors, a $2|F_o| - |F_c|$ map showed electron density clearly defining each inhibitor. Further conventional isotropic refinement, adopting rigid-body for the inhibitor and including successively water molecules, resulted in a model with R, R_{free} of 0.185, 0.232 and 0.204, 0.243 for MMP-8:FLTP and MMP-8:TIC, respectively. At this stage the refinement was continued with SHELXL[59] adopting restrained conjugate-gradient least-squares minimization. After each step of about 10 cycles, electron density maps were calculated, the model was rebuilt if necessary using the program O,[60] and new peaks were added as water molecules after manual checking. Further refinement treating non-H atoms anisotropically, including H atoms at calculated positions, and adding more residues in multiple conformations resulted in the final model. Summary of the refinement statistics is given in Table 3. The refined atomic coordinates will be deposited with the Protein Data Bank.

Acknowledgment. We thank Prof. M. Paglialunga Paradisi for the NMR spectra. This work was partly supported by funds from MURST, Program Cofin 97 CFSIB, from CNR, Targeted Program Biotecnologie, and from the Deutsche Forschungsgemeinschaft, Bonn, Project Ts/35-2. One of us (E.G.) gratefully acknowledges grants from Deutsche Forschungsgemeinschaft (DFG) and Consiglio Nazionale delle Ricerche (CNR) for a study leave at EMBL c/o DESY (Hamburg).

References

(1) Pyke, C.; Ralfkiaer, E.; Huhtala, P.; Hurskainen, T.; Dano, K.; Tryggvason, K. Localization of messenger RNA for M_r 72,000 and 92,000 type IV collagenases in human skin cancers by *in situ* hybridization. *Cancer Res.* **1992**, *52*, 1336−1341.

(2) Gijbels, K.; Masure, S.; Carton, H.; Opdenakker, G. Gelatinase in the cerebrospinal fluid of patients with multiple sclerosis and other inflammatory neurological disorders. *J. Neuroimmunol.* **1992**, *41*, 29−34.

(3) Walakovits, L. A.; Moore, V. L.; Bhardwaj, N.; Gallick, G. S.; Lark, M. W. Detection of stromelysin and collagenase in synovial fluid from patients with rheumatoid arthritis and posttraumatic knee injury. *Arthritis Rheumatism* **1992**, *35*, 35−42.

(4) Beckett, R. P.; Whittaker, M**.** Matrix metalloproteinase inhibitors 1998. *Exp. Opin. Ther. Patents* **1998**, *8*, 259−282.

(5) Hodgson, J. Remodeling MMPIs. Matrix metalloproteinase inhibitors will be approved as drugs, probably this year, but questions remain concerning their specificity, bioavailability, and potential long-term toxicity. *Biotechnology* **1995**, *13*, 554−557.

(6) Grams, F.; Dive, V.; Yiotakis, A.; Yiallouros, I.; Vassiliou, S.; Zwilling, R.; Bode, W.; Stöcker, W. Structure of astacin with a transition-state analogue inhibitor. *Nat. Struct. Biol.* **1996**, *3*, 671−675.

(7) Vassiliou, S.; Mucha, A.; Cuniasse, P.; Georgiadis, D.; Lucet-Levannier, K.; Beau, F.; Kannan, R.; Murphy, G.; Knäuper, V.; Rio, M.-C.; Basset, P.; Yiotakis, A.; Dive, V. Phosphinic pseudotripeptides as potent inhibitors of matrix metalloproteinanses: a structure−activity study. *J. Med. Chem.* **1999**, *42*, 2610−2620.

(8) Cirilli, M.; Gallina, C.; Gavuzzo, E.; Giordano, C.; Gomis-Rüth, F. X.; Gorini, B.; Kress, L. F.; Mazza, F.; Paglialunga Paradisi, M.; Pochetti, G.; Politi, V. 2 Å X-ray structure of adamalysin II complexed with a peptide phosphonate inhibitor adopting a retro-binding mode. *FEBS Lett.* **1997**, *418*, 319−322.

(9) D'Alessio, S.; Gallina, C.; Gavuzzo, E.; Giordano, C.; Gorini, B.; Mazza, F.; Paglialunga Paradisi, M.; Panini, G.; Pochetti, G.; Sella, A. Inhibition of adamalysin II and MMPs by phosphonate analogues of snake venom peptides. *Bioorg. Med. Chem. Lett.* **1999**, *7*, 389−394.

(10) Gomis-Rüth, F. X.; Meyer, E. F.; Kress, L. F.; Politi, V.. Structures of adamalysin II with peptidic inhibitors. Implications for the design of tumor necrosis factor α convertase inhibitors. *Protein Sci.* **1998**, *7*, 283−292.

(11) Gallina, C.; Gavuzzo, E.; Giordano, C.; Gorini, B.; Mazza, F.; Paglialunga Paradisi, M.; Panini, G.; Pochetti, G.; Politi, V. Phosphonate inhibitors of adamalysin II and matrix metalloproteinases. *Ann. N. Y. Acad. Sci.* **1999**, *878*, 700−702.

(12) Thorwart, W.; Schwab, W.; Schudok, M.; Haase, B.; Bartnik, E.; Weithmann, K.-U. Cyclic and heterocyclic N-substituted α-iminohydroxamic and carboxylic acids. PCT Int. Appl. WO 97/18194, 1997.

(13) Matter, H.; Knauf, M.; Schwab, W.; Paulus, E. F. Relative configuration and conformation of key intermediates for matrix metalloproteinase inhibitors as determined by NMR-based restrained simulated annealing and validated by X-ray anlysis. *J. Am. Chem. Soc.* **1998**, *120*, 11512−11513.

(14) Kazmierski, W. M.; Hruby, V. J. A new approach to receptor ligand design: synthesis and conformation of a new class of potent and highly selective μ opioid antagonists utilizing tetrahydroisoquinoline carboxylic acid. *Tetrahedron* **1988**, *44*, 697−710.

(15) Kazmierski, W.; Wire, W. S.; Lui, G. K.; Knapp, R. J.; Shook, J. E.; Burks, T. F.; Yamamura, H. I.; Hruby, V. J. Design and synthesis of somatostatin analogues with topographical properties that lead to highly potent and specific μ opioid receptor antagonists with greatly reduced binding at somatostatin receptors. *J. Med. Chem.* **1988**, *31*, 2170−2177.

(16) Kazmierski, W. M.; Yamamura, H. I.; Hruby, V. J. Topographic design of peptide neurotransmitters and hormones on stable backbone templates: relation of conformation and dynamics to bioactivity. *J. Am. Chem. Soc.* **1991**, *113*, 2275−2283.

(17) Valle, G.; Kazmierski, W. M.; Crisma, M.; Bonora, G. M.; Toniolo, C.;, Hruby, V. J. Constrained phenylalanine analogues. Preferred conformation of the 1,2,3,4-tetrahydroisoquinoline-3-carboxylic acid (Tic) residue. *Int. J. Pept. Protein Res.* **1992**, *40*, 222−232.

(18) Kazmierski, W. M.; Urbanczyk-Lipkowska, Z.; Hruby, V. J. New amino acids for the topographical control of peptide conformation: synthesis of all the isomers of α,*β*-dimethylphenylalanine and α,*β*-dimethyl-1,2,3,4-tetrahydroisoquinoline-3-carboxylic acid of high optical purity. *J. Org. Chem.* **1994**, *59*, 1789−1795.

(19) Josien, H.; Lavielle, S.; Brunissen, A.; Saffroy, M.; Torrens, Y.; Beaujouan, J.-C.; Glowinski, J.; Chassaing, G. Design and synthesis of side-chain conformationally restricted phenylalanines and their use for structure−activity studies on tackykinin NK-1 receptor. *J. Med. Chem.* **1994**, *37*, 1586−1601.

(20) Sawutz, D. G.; Salvino, J. M.; Seoane, P. R.; Douty, B. D.; Houck, W. T.; Bobko, M. A.; Doleman, M. S.; Dolle, R. E.; Wolfe, H. R. Synthesis, characterization, and conformational analysis of the D/L-Tic stereoisomers of the bradykinin receptor antagonist D-Arg^0[Hyp^3,Thi^5,D-Tic^7,Oic^8] bradykinin. *Biochemistry* **1994**, *33*, 2373−2379.

(21) Dery, O.; Josien, H.; Grassi, J.; Chassaing, G.; Couraud, J. Y.; Lavielle, S. Use of conformationally constrained peptides for a topographical analysis of the combining site of a monoclonal antisubstance P antibody. *Biopolymers* **1996**, *39*, 67−74.

(22) Levy, D. E.; Lapierre, F.; Liang, W.; Ye, W.; Lange, C. W.; Li, X.; Grobelny, D.; Casabonne, M.; Tyrrell, D.; Holme, K.; Nadzan, A.; Galardy, R. E. Matrix metalloproteinase inhibitors: a structure−activity study. *J. Med. Chem.* **1998**, *41*, 199−223.

(23) Calcagni, A.; Gavuzzo, E.; Lucente, G.; Mazza, F.; Pochetti, G.; Rossi, D. Structure and conformation of peptides containing the sulfonamide junction. *Int. J. Pept. Protein Res.* **1989**, *34*, 319−324.

(24) Zecchini, G.; Paradisi, M. P.; Torrini, I.; Lucente, G.; Gavuzzo, E.; Mazza, F.; Pochetti, G. Retrosulfonamido peptide analogues. Synthesis and crystal conformation of Boc-Pro-Leu-Ψ(NH-SO_2)-Gly-NH_2. *Tetrahedron Lett.* **1991**, *32*, 6779−6782.

(25) Calcagni, A.; Gavuzzo, E.; Mazza, F.; Pinnen, F.; Pochetti, G.; Rossi, D. Structure and conformation of peptides containing the sulfonamide junction. IV. Synthesis and crystal conformation of N-benzoyl-L-phenylalanyl-tauryl-L-leucine methyl ester. *Gazz. Chim. Ital.* **1992**, *122*, 17−23.

(26) Calcagni, A.; Rossi, D.; Paglialunga Paradisi, M.; Lucente, G.; Luisi, G.; Gavuzzo, E.; Mazza, F.; Pochetti, G.; Paci, M. Peptides containing the sulfonamide junction: synthesis, structure, and conformation of Z-Tau-Pro-Phe-NHiPr. *Biopolymers* **1997**, *41*, 555−567.

(27) Matter, H.; Schwab, W.; Barbier, D.; Billen, G.; Haase, B.; Neises, B.; Schudok, M; Thorwart, W.; Schreuder, H.; Brachvogel, V.; Lönze, P.; Weithmann, K. U. Quantitative structure−activity relationship of human neutrophil collagenase (MMP-8) inhibitors using comparative molecular field analysis and X-ray structure analysis. *J. Med. Chem.* **1999**, *42*, 1908−1920.

(28) Powers, J. C.; Harper, J. W. Inhibitors of metalloproteases. In *Proteinase Inhibitors*; Barrett, A. J., Salvesen, G., Eds.; Elsevier Science Publishers: Amsterdam, 1986; pp 219−298.

(29) König, W.; Geiger, R. A new method for synthesis of peptides: activation of the carboxyl group with dicyclohexylcarbodiimide using 1-hydroxybenzotriazoles as additives. *Chem. Ber.* **1970**, *103*, 788−798.

(30) Solas, D.; Hale, R. L.; Patel, D. V. An efficient synthesis of *N*-α-Fmoc-4-(phosphonodifluoromethyl)-*L*-phenylalanine. *J. Org. Chem.* **1996**, *61*, 1537−1539.

(31) Lavielle, G.; Hantefaye, P.; Schaeffer, C.; Boutin, J. A.; Cudennec, C. A.; Pierré, A. New α-amino phosphonic acid derivatives of vinblastine: chemistry and antitumor activity. *J. Med. Chem.* **1991**, *34*, 1998−2003.

(32) Bode, W.; Reinemer, P.; Huber, R.; Kleine, T.; Schnierer, S.; Tschesche, H. The X-ray crystal structure of the catalytic domain of human neutrophil collagenase inhibited by a substrate analogue reveals the essentials for catalysis and specificity. *EMBO J.* **1994**, *13*, 1263−1269.

(33) Reinemer, P.; Grams, F.; Huber, R.; Kleine, T.; Schnierer, S.; Pieper, M.; Tschesche, H.; Bode, W. Structural implications for the role of the N terminus in the "superactivation" of collagenases. *FEBS Lett.* **1994**, *338*, 227−233.

(34) Grams, F.; Reinemer, P.; Powers, J. C.; Kleine, T.; Pieper, M.; Tschesche, H.; Huber, R.; Bode, W. X-ray structures of human neutrophil collagenase complexed with peptide hydroxamate and peptide thiol inhibitors. Implications for substrate binding and rational drug design. *Eur. J. Biochem.* **1995**, *228*, 830−841.

(35) Lovejoy, B.; Cleasby, A.; Hassell, A. M.; Longley, K.; Luther, M. A.; Weigl, D.; McGeehan, G.; McElroy, A. B.; Drewry, D.; Lambert, M. H.; Jordan, S. R. Structure of the catalytic domain of fibroblast collagenase complexed with an inhibitor. *Science* **1994**, *263*, 375−377.

(36) Becker, J. W.; Marcy, A. I.; Rokosz, L. L.; Axel, M. G.; Burbaum, J. J.; Fitzgerald, P. M. D.; Cameron, P. M.; Esser, C. K.; Hagmann, W. K; Hermes, J. D.; Springer, J. P. Stromelysin-1: three-dimensional structure of the inhibited catalytic domain and of the C-truncated proenzyme. *Protein Sci.* **1995**, *4*, 1966−1976.

(37) Stams, T.; Spurlino, J. C.; Smith, D. L.; Wahl, R. C.; Ho, T. F.; Qoronfleh, M. W.; Banks, T. M.; Rubin, B. Structure of human neutrophil collagenase reveals large S'_1 specificity pocket. *Nat. Struct. Biol.* **1994**, *1*, 119−123.

(38) Grams, F.; Crimmin, M.; Hinnes, L.; Huxley, P.; Pieper, M.; Tschesche, H.; Bode, W. Structure determination and analysis of human neutrophil collagenase complexed with a hydroxamate inhibitor. *Biochemistry* **1995**, *34*, 14012−14020.

(39) Betz, M.; Huxley, P.; Davies, S. J.; Mushtaq, Y.; Pieper, M.; Tschesche, H.; Bode, W.; Gomis-Rüth, F. X. 1.8-Å crystal structure of the catalytic domain of human neutrophil collagenase (matrix metalloproteinase-8) complexed with a peptidomimetic hydroxamate primed-side inhibitor with a distinct selectivity profile. *Eur. J. Biochem.* **1997**, *247*, 356−363.

(40) Brandstetter, H.; Engh, R. A.; Graf Von Roedern, E.; Moroder, L.; Huber, R.; Bode, W.; Grams, F. Structure of malonic acid-based inhibitors bound to human neutrophil collagenase. A new binding mode explains apparently anomalous data. *Protein Sci.* **1998**, *7*, 1303−1309.

(41) Morphy, J. R.; Milican, T. A.; Porter, J. R. Matrix metalloproteinase inhibitors: current status. *Curr. Med. Chem.* **1995**, *2*, 743−762.

(42) Hajduk, P. J.; Sheppard, G.; Nettesheim, D. G.; Olejniczak, E. T.; Shuker, S. B.; Meadows, R. P.; Steinman, D. H.; Carrera, G. M. Jr.; Marcotte, P. A.; Severin, J.; Walter, K.; Smith, H.; Gubbins, E.; Simmer, R.; Holzman, T. F.; Morgan, D. W.; Davidsen, S. K.; Summers, J. B.; Fesik, S. W. Discovery of potent nonpeptide inhibitors of stromelysin using SAR by NMR. *J. Am. Chem. Soc.* **1997**, *119*, 5818−5827.

(43) Schmitt, J. D.; Sharples, C. G. V.; Caldwell, W. S. Molecular recognition in nicotinic acethylcholine receptors: the importance of *π*-cation interactions. *J. Med. Chem.* **1999**, *42*, 3066−3074.

(44) Aoki, K.; Murayama, K.; Nishiyama, H.; Cation-*π* interaction between the trimethylammonium moiety and the aromatic ring within indole-3-acetic acid choline ester, a model compound for molecular recognition between acetylcholine and its esterase: an X-ray study. *J. Chem. Soc., Chem. Commun.* **1995**, *331*, 2221−2222.

(45) Dougherty, D. A. Cation-*π* interactions in chemistry and biology: a new view of benzene, Phe, Tyr, and Trp. *Science* **1996**, *271*, 163−168.

(46) Ma, J. C.; Dougherty, D. A. The cation-*π* interaction. *Chem. Rev.* **1997**, *97*, 1303−1324.

(47) Nicklaus, M. C.; Neamati, N.; Hong, H.; Mazumder, A.; Sunder, S.; Chen, J.; Milne, G. W. A.; Pommier, Y. HIV-1 integrase pharmacophore: discovery of inhibitors through three-dimensional database searching. *J. Med. Chem.* **1997**, *40*, 920−929.

(48) Babine, R. E.; Bender, S. Molecular recognition of protein−ligand complexes: applications to drug design. *Chem. Rev.* **1997**, *97*, 1359−1472.

(49) Ashida, T.; Tsunogae, Y.; Tanaka, I.; Yamane, T. Peptide chain structure parameters, bond angles and conformational angles from the Cambridge Structural Database. *Acta Crystallogr.* **1997**, *B43*, 212−218.

(50) Allen, F. H.; Bellard, S.; Brice, M. D.; Cartwright, B. A.; Doubleday, A.; Higgs, H.; Hummelink, T.; Hummelink-Peters, B. G.; Kennard, O.; Motherwell, W. D. S.; Rodgers, J. R.; Watson, D. G. The Cambridge crystallographic data center: computer-based search, retrieval, analysis and display of information. *Acta Crystallogr.* **1979**, *B35*, 2331−2339.

(51) Stöcker, W.; Grams, F.; Baumann, U.; Reinemer, P.; Gomis-Rüth, F. X.; McKay, D. B.; Bode, W. The metzincins. Topological and sequential relations between the astacins, adamalysins, serralysins, and matrixins (collagenases) define a superfamily of zinc-peptidases. *Protein Sci.* **1995**, *4*, 823−840.

(52) Netzel-Arnett, S.; Fields, G. B.; Birkedal-Hansen, H.; van Wart, H. E. Sequence specificities of human fibroblast and neutrophil collagenases. *J. Biol. Chem.* **1991**, *266*, 6747−6755.

(53) Niedzwiecki, L.; Teahan, J.; Harrison, R. K.; Stein, R. L. Substrate specificity of the human matrix metalloproteinase stromelysin and the development of continuous fluorometric assays. *Biochemistry* **1992**, *31*, 12618−12623.

(54) Netzel-Arnett, S.; Sang, Q.-X.; Moore, W. G. I.; Navre, M.; Birkedal-Hansen, H.; van Wart, H. E. Comparative sequence specificities of human 72- and 92-kDa gelatinases (type IV collagenases) and PUMP (matrilysin). *Biochemistry* **1993**, *32*, 6427−6432.

(55) Krumme, D.; Wenzel, H.; Tschesche, H. Hydroxamate derivatives of substrate-analogous peptides containing aminomalonic acid are potent inhibitors of matrix metalloproteinases. *FEBS Lett.* **1998**, *436*, 209−212.

(56) Schnierer, S.; Kleine, T.; Gote, T.; Hillemann, A.; Knäuper, V.; Tschesche, H. The recombinant catalytic domain of human neutrophil collagenase lacks type I collagen substrate specificity. *Biochem. Biophys. Res. Commun.* **1993**, *191*, 319−326.
(57) Otwinowski, Z.; Minor, W. Processing of X-ray diffraction data collection in oscillation mode. *Methods Enzymol.* **1997**, *276*, 307−326.
(58) Brünger, A. T. *X-PLOR, version 3.1, A system for X-ray crystallography and NMR*; Yale University Press: New Haven, CT, 1992.
(59) Sheldrick, G. M.; Schneider, T. R. SHELXL: high-resolution refinement. *Methods Enzymol.* **1997**, *277*, 319−343.
(60) Jones, T. A.; Zou, J. Y.; Cowan, S. W.; Kjeldgaard, M. Improved methods for building protein models in electron density maps and the location of errors in these models. *Acta Crystallogr.* **1991**, *A47*, 110−119.

JM9909589